Sensors & Actuators: B. Chemical 329 (2021) 129037

Contents lists available at ScienceDirect

Sensors and Actuators: B. Chemical

journal homepage: www.elsevier.com/locate/snb

Machine learning-based colorimetric determination of glucose in artificial saliva with different reagents using a smartphone coupled μPAD

Öykü Berfin Mercan [a], Volkan Kılıç [a,*], Mustafa Şen [b,*]

[a] Electrical and Electronics Engineering Graduate Program, Izmir Katip Celebi University, Izmir, Turkey
[b] Department of Biomedical Engineering, Izmir Katip Celebi University, Izmir, Turkey

ARTICLE INFO

Keywords:
Image processing
Colorimetry
Machine learning
Smartphone
Android application
Paper-based sensors
Glucose
μPAD

ABSTRACT

Potassium iodide (KI) and 3,3′,5,5′-tetramethylbenzidine (TMB) are frequently used as chromogenic agents in μPADs for glucose determination. Chitosan (Chi) has peroxidase like activity and improves the analytic performance of μPADs when used in combination with a chromogenic agent. Here, a portable platform incorporating a μPAD with a smartphone application based on machine learning was developed to quantify glucose concentration in artificial saliva. The detection zones of the μPAD were modified with three different detection mixtures containing; (i) KI, (ii) KI+Chi and (iii) TMB. After the color change, the images of the μPADs were taken with four different smartphones under seven different illumination conditions. The images were first processed for feature extraction and then used to train machine learning classifiers, resulting in a more robust and adaptive platform against illumination variation and camera optics. Different machine learning classifiers were tested and the best machine learning classifier for each detection mixture was obtained. Next, a special application called "*Gluco-Sensing*" capable of image capture, cropping and processing was developed to make the system more user-friendly. A cloud system was used in the application to communicate with a remote server running machine learning classifiers. Among the three different detection mixtures, the mixture with TMB demonstrated the highest classification accuracy (98.24%) with inter-phone repeatability under versatile illumination.

1. Introduction

Paper-based microfluidic devices (μPAD) have been extensively studied as novel analytical tools for a variety of applications ranging from environmental monitoring to point-of-care diagnostic tests since their first introduction [1]. μPADs have many attractive qualities such as being disposable, practical, low-cost, and user-friendly [2]. Millions of people die every year from preventable diseases and for that providing cheap and accessible healthcare alternatives especially to countries with limited resources is essential to improve the quality of life. The World Health Organization (WHO) outlined all the criteria required for a device to be used in developing countries and they are abbreviated as "ASSURED"; affordable, sensitive, specific, user-friendly, rapid and robust, equipment-free and deliverable to end-users [3,4]. μPADs have the potential to meet all these specified criteria. These devices can be made very small and don't need any power for operation. μPADs are typically made by patterning a paper with a hydrophobic-ink using various techniques (e.g. stamping [5], plasma treatment [6] and wax [7, 8], screen [9] and inkjet [10] printing) to create hydrophobic barriers. These barriers facilitate the confinement and flow of samples and reagents to predefined locations via capillary force without the use of external equipment. In order to perform a rapid, sensitive and selective analysis, a variety of detection principles including chemiluminescence, fluorescence, electrochemical and colorimetric detection have been used in μPADs [11–13]. Among them, colorimetric detection has attracted more attention as it requires no sophisticated tool for qualitative analysis [14]. Basically, the molecule of interest causes a color change in the detection zone for a visual readout.

The colorimetric analysis finds applications in many fields including food allergen testing [15], albumin testing in urine analysis [16], blood analysis [17], pH quantification [18], and water monitoring [19]. The color information in paper-based sensors could be collected in various color spaces such as RGB (Red-Green-Blue), HSV (Hue-Saturation-Value) and L*a*b* (Lightness, Green-Red, Blue-Yellow) [18, 20–22]. There are numerous reports using these color spaces for the detection of a variety of chemicals. For example, HSV color space converted from RGB was used for the detection of alcohol in saliva and a model textile dye (BR9) [23,24] while L*a*b* color space was used for

* Corresponding author.
E-mail addresses: volkan.kilic@ikcu.edu.tr (V. Kılıç), mustafa.sen@ikcu.edu.tr (M. Şen).

https://doi.org/10.1016/j.snb.2020.129037
Received 10 July 2020; Received in revised form 11 October 2020; Accepted 12 October 2020
Available online 24 October 2020

sensitive pH measurement in the range of 1–12 [25]. RGB color space itself was employed for the detection of chlorine in water [26] and ripeness estimation of fruits [27] where the colorimetric analysis was performed with analytical expression based on color space parameters. However, colorimetric analysis is highly affected by ambient light conditions and camera optics. To address this issue, advanced algorithms such as machine learning were proposed in the quantitative evaluation process [18,28]. With its powerful utilities like automated decision-making and self-learning from the data, machine learning became a current trend in the field of statistical analysis. It seems that machine learning will be the dominant method for a long time due to its flexibility and adaptability to new platforms such as smartphone-based systems. With the recent advances in smartphone technology, numerous platforms capable of running sophisticated algorithms have been developed that can perform colorimetric analysis for reliable qualitative and quantitative evaluations of colorimetric assays. In [29,23], *SPAQ* application was developed to test the alcohol level in saliva based on histogram distribution. To detect pH, protein, and glucose values in an assay, *Colorimetric Test Reader* application was reported in [30]. *Colorimetric Plate Reader* application for ELISA tests was developed in [31]. *PhotoMetrix* was developed in [32] to quantify the analytes in the samples employing the univariate and multivariate analyses. *ChemTrainer* application [28] was proposed which sends the captured image to the remote server via cloud systems in order to process with machine learning classifiers. Despite the increasing popularity, smartphone-based colorimetric quantification has some obvious issues including reliability, accessories and simplicity. The result obtained in the smartphone application should be explicit and accurate in any circumstances. In [30–32], a calibration curve was derived based on measurements in a controlled environment. Even if they work accurately in a controlled environment, results may deviate when the test is performed under different conditions than the controlled environment. They are also sensitive to smartphone brands and camera optics. To prevent outer interference, custom accessories designed in 3D printer were used which may not be convenient for the users [23,31]. In addition, the application should be operable in the field without extensive training, requiring them to have a simple and user-friendly interface. Therefore, we proposed a new platform which is robust and adaptive to illumination variance without any accessories, gives accurate results regardless of the smartphone brand and have a simple interface that even non-expert users may use without training.

In recent years, a great deal of focus has been given to the development of measurement systems that detect glucose non-invasively and reliably in other bodily fluids including saliva, sweat and tear as an alternative to measuring blood glucose level invasively from a drop of blood [33]. In our recent study, a μPAD was integrated with a portable smartphone-based platform for rapid, sensitive, selective and quantitative detection of glucose in artificial saliva [34]. The platform runs under our custom-design Android application (*GlucoSense*) capable of offline (without internet access) image processing and analysis to provide a rapid colorimetric evaluation of glucose based on a calibration curve. In order to eliminate the interference of ambient light, a custom-designed 3D printed case was integrated with a smartphone, which might not be practical in daily use. Here, machine learning classifiers were integrated with the system to freely use the platform under ambient light without any restriction. The use of the machine learning simplified the platform and improved its robustness and adaptability. A dataset was created under three light sources with four different smartphones to train machine learning classifiers and thus to improve the platform against the illumination variance and camera optics. In addition, *GlucoSense* was upgraded to be able to send the data to the server via a cloud system that run the proposed machine learning classifiers. The proposed integrated platform has a great prospect for glucose determination in non-laboratory and resource-limited settings.

2. Experimental setup

2.1. Materials

Phosphate buffered saline (PBS) (Sigma Aldrich, USA), 3,3′,5,5′-tetramethylbenzidine (TMB) (Sigma Aldrich, USA), potassium chloride (KCl) (Sigma Aldrich, USA), potassium iodide (KI) (Sigma Aldrich, USA), chitosan (Chi) – low molecular weight (Sigma Aldrich, USA), acetic acid – 2% (v/v) in H_2O (Sigma Aldrich, USA), D(+)-glucose ($C_6H_{12}O_6$) ≥99.5%, glucose oxidase from Aspergillus niger (211 U/mg) (Sigma Aldrich, USA), peroxidase from horseradish (HRP, 325 U/mg) (Sigma Aldrich, USA), Whatman qualitative filter paper – grade 1 (Sigma Aldrich, USA), artificial saliva (NeutraSal, Germany). All chemicals were used as received and prepared using MilliQ-water except TMB throughout the study. TMB was dissolved in ethanol.

2.2. Fabrication of μPAD

μPADs were made using wax printing [7,8]. A pattern was designed on Microsoft-PowerPoint 2013 Software and printed on Whatman filter paper using a wax printer (Xerox ColorQube 8900, Xerox Corporation, USA). Subsequently, the paper with the designed patterns was placed on a hot plate at 180 °C for 120 s simply to melt the printed wax and create the hydrophobic barriers that define the channels and the detection zones. The detection zones of the μPADs were modified as shown in Fig. 1. Briefly, an enzyme mixture containing 180 U/ml GOx and 50 U/ml HRP was prepared in PBS at pH 7. Then, 1 μl aliquots of the

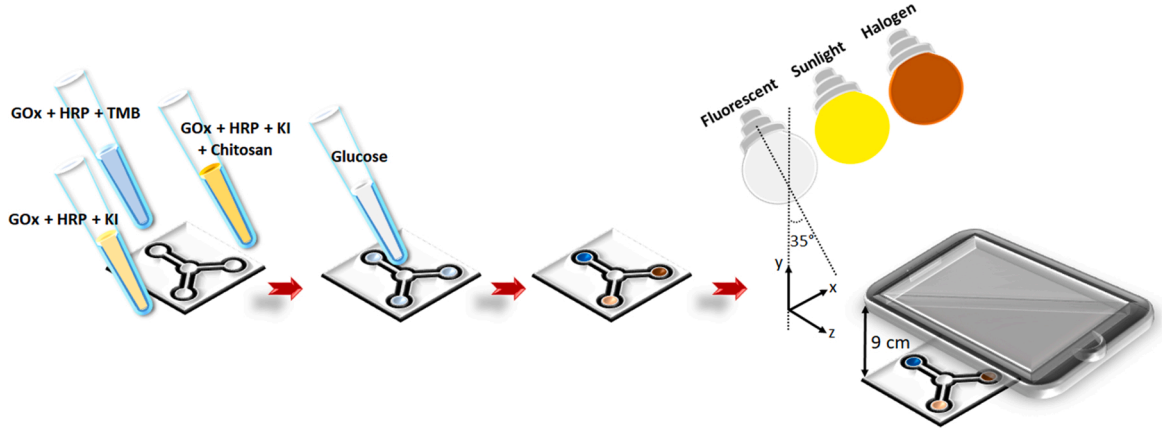

Fig. 1. Schematic illustration of the glucose determination strategy. The change in color in the detection zones of the μPAD was imaged using a smartphone camera under various combinations of fluorescent, halogen and sunlight sources.

mixture were carefully and slowly dropped on all three detection zones of μPADs. Next, 1 μl of 3 mM KI was dropped onto two of the detection zones and 1 μl of 10 mM TMB onto the remaining detection zone. The solutions were left to dry for about 5 min at room temperature. Following that 1 μl of 1% (w/v) Chi was dropped onto one of the two detection zones with KI. Next, one side of the μPADs was sealed with a transparent tape to prevent solution leakage. The colorimetric behavior of μPAD was assessed using artificial saliva with glucose. Basically, 15 μl aliquots of test solutions containing glucose at varying concentrations (0.1, 0.25, 0.5, 0.75, 1, 5 and 10) were introduced into the sample insertion regions of μPADs and allowed to reach all three detection zones under lateral flow.

2.3. Image capturing

Machine learning based approaches need to be trained with a prior dataset to achieve high classification performance. Contents of a dataset are directly linked to the classifier performance which could be readily improved with the number of input data including adverse effects such as ambient illumination conditions and camera optics. Therefore, a dataset was created with multiple smartphones to imitate the adverse effects under controlled illumination conditions using halogen (H), fluorescent (F) and sunlight (S) light bulb sources. Individual and combination of light sources were used to create seven light conditions: H, F, S, HF, HS, FS, HFS to capture the image of each μPAD concentration. The halogen (Osram 60 W) light bulb provides warm (2700 K) colors while the fluorescent (Klite 6 W) and sunlight (Philips 5.5 W) bulbs emit neutral (4000 K) and cool colors (6500 K), respectively. Although more illumination sources can be included to extend the dataset, three sources are found to be adequate based on extensive experimental studies. The images of μPADs were captured under a homogeneously illuminated field at 35° angle of incidence with a constant distance of 9 cm between smartphones and μPADs. The position of μPADs, the light sources and the smartphones were fixed in a closed box to ensure that the angle of incidence and the distance between smartphones and μPADs remain the same for all test groups.

As the smartphones are equipped with distinctive camera, optics and imaging software, images are quite diverse even under controlled illumination conditions. Table 1 presents two Android (Reeder P10 and Samsung J7) and two iOS (iPhone 6S and iPhone 7) smartphones with their properties used in this study. The positioning and height of the smartphones were kept the same in capturing each μPAD image for all illuminations and concentrations. The automatic mode was used to let the embedded imaging software adjust the settings such as color temperature, ISO, exposure time and shutter speed. Eight concentrations under seven illumination conditions lead to having 56 images for each smartphone, resulting in 224 images for the whole dataset.

This dataset was then transferred to a computer for further processing with MATLAB (R2019a, MathWorks Inc.). The region of interest (ROI) is the region where the color change occurs due to the reaction of the mixtures. To extract the ROI, several image processing methods need to be applied sequentially including grayscale conversion, thresholding, binarizing, masking, contour detection and noise removal. The extracted ROI was then masked with original images to extract the features for machine learning.

Table 1
The smartphones used to create a dataset with images of μPADs for machine learning.

Smartphone brand	Image resolution	Optics	Focal length
iPhone 6S	4032 × 3024	$f/2.2$	4 mm
iPhone 7	4032 × 3025	$f/1.8$	4 mm
Reeder P10	4160 × 3120	$f/2$	4 mm
Samsung J7	4128 × 2322	$f/1.9$	4 mm

2.4. Machine learning

To identify and detect the correlation between the color change and concentration, seventeen machine learning classifiers were trained and evaluated in terms of their ability to precisely predict the glucose concentration from the colorimetric ranks of different reagents. Among the tested classifiers, the ones with the best performance for each mixture were identified and integrated with the smartphone-based platform. The identified classifiers are linear discriminant analysis (LDA) [35], gradient boosting classifier (GBC) [36] and random forest (RF) [28].

The LDA is a supervised classification technique that estimates the mean and variance from the data for each class. To make predictions, Bayesian rule is employed to calculate the highest likelihood for the input data among all classes using discriminant function under the assumption that all classes have equal co-variance. This assumption leads to having linear terms in discriminant function which gives the name to the technique as LDA. The GBC utilizes an ensemble of weak prediction models to build an enhanced prediction based on decision trees. The decision trees are joined to the ensemble one at a time in order to minimize the prediction errors caused by previous models. Similarly, the RF classifier constructs a prediction model in the form of an ensemble of individual decision trees. The prediction is based on voting the outputs generated by employing decision trees on randomly selected data samples.

To train the classifiers, color and texture features were extracted after image processing. Firstly, RGB values of the image were converted to HSV and L*a*b* to analyze the effect of color spaces on concentration level. Then, mean, skewness and kurtosis values were calculated for each R, G, B, H, S, V, L*, a*, b* color channels. Along with the color features, texture features were also extracted to improve the accuracy of the classifiers. Texture features, namely, contrast, correlation, homogeneity and energy, are statistical features based on intensity and color transition of images [37]. In addition to color and texture features, entropy and intensity values of images were calculated. Totally, 33 features were used to train the classifiers in Python programming language.

In machine learning, k-fold cross-validation is a popular technique to evaluate the performance of the classifiers which splits the dataset into k equal folds [38]. Then, $k-1$ number of folds are used for training of model and the remaining fold is used to test the trained model. This process is repeated k iterations. Thus, the different fold is used as a training and testing set in each iteration, resulting in k different accuracy values. The average of these values is used to calculate the overall accuracy of the classifier. Here, k is set to 10 which was reported to be adequate to avoid issues caused by high bias and variance [39].

2.5. Smartphone application: GlucoSensing

We upgraded our custom-designed Android application *GlucoSense* [34] for colorimetric determination of glucose in μPADs with machine learning and named it as *GlucoSensing*. In the first version, *GlucoSense* was developed with a simple and user-friendly interface capable of image processing without an internet connection. The current version *GlucoSensing* was developed with new features to address the feedback from *GlucoSense*, resulting in its improvement in terms of simplicity, robustness and user-friendliness. The most important feature of *GlucoSensing* is the ability to communicate with the remote server via cloud connection to be able to benefit the advantage of machine learning. The communication between the *GlucoSensing* and the server is based on the Firebase cloud system which supports both Android and Python platforms. The Firebase stores communication settings as JSON (Javascript Object Notation) format. JSON files are added to both Android and Python libraries to set communication protocols between them. The present platform supports any operating system (Windows, Mac OSX or Linux) running Python version over 3.6 as a server. The proposed classifiers running in Python communicates with the Firebase to receive the images or transmit the classification results. The *GlucoSensing* is

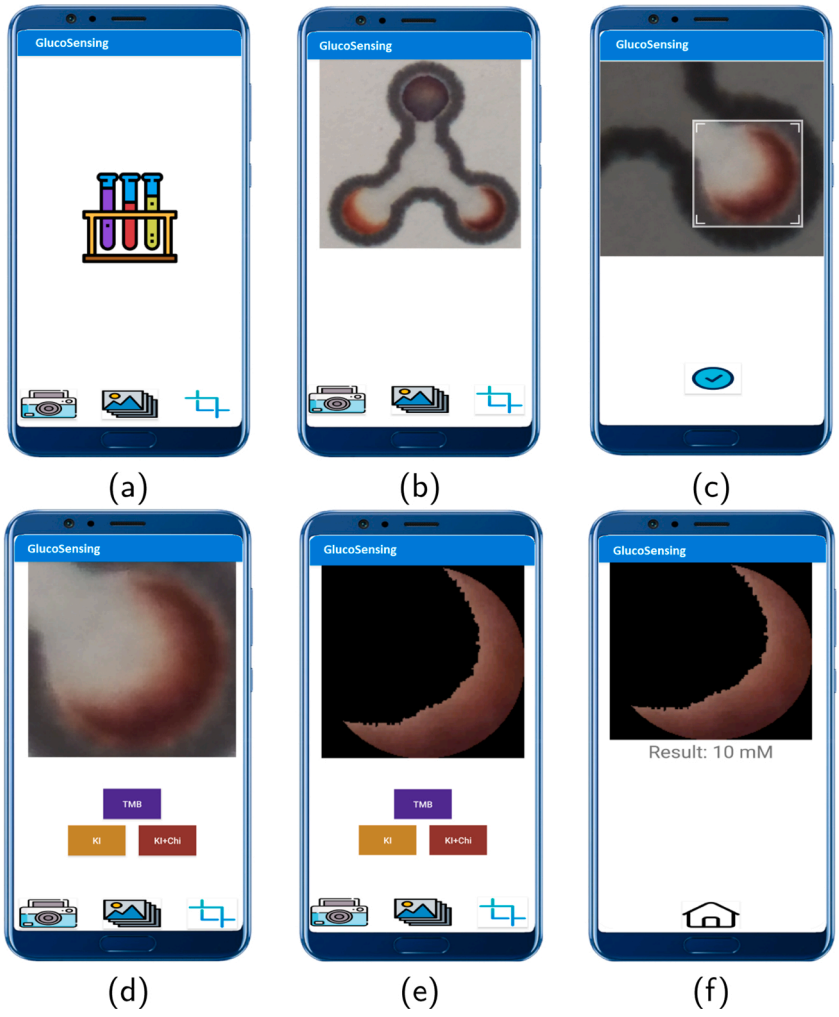

Fig. 2. Colorimetric glucose quantification steps on the *GlucoSensing*. The homepage of the *GlucoSensing* is given in (a). The user can select an image from the gallery or capture a new image using the smartphone camera and display it on the screen as in (b). The image can be cropped using an adjustable cropbox in (c). The cropped patch is given in (d) and the ROI after the image processing is shown in (e). The classification result of the image is given in (f).

implemented in Android studio supporting version 8 (Oreo) and above. The *GlucoSensing* allows the user to take a new image using the smartphone camera or load an image from the gallery as shown in Fig. 2a. The selected image can be cropped in circular using an adjustable cropbox to narrow down the area for the ROI search (Fig. 2b and c). When the "TMB, KI or KI+Chi" buttons are tapped, the ROI in the cropped image is obtained by image processing (Fig. 2d and e). *GlucoSensing* sends the ROI to the server and the machine learning classifiers in the server run to decide the class of μPAD with respect to its color and texture features. The result is sent back to the *GlucoSensing* over the Firebase to be displayed on the screen as shown in Fig. 2f.

3. Results and discussion

Glucose oxidase/peroxidase method in combination of various indicators was used for the determination of glucose in artificial saliva. First, μPADs with three detection zones were fabricated using wax printing. Then, all three detection zones of the μPADs were modified with detection mixtures containing (i) KI, (ii) KI+Chi, and (iii) TMB, respectively. All detection mixtures contained GOx and HRP enzymes. For colorimetric determination of glucose, GOx catalyzes the oxidation of β-D-glucose to D-glucono-1,5-lactone and produces H_2O_2 as a by-product [40]. HRP uses the by-product H_2O_2 to catalyze the conversion of either KI or TMB and thus causes a visible color change. Chi has been shown to have peroxidase-like activity [41] where H_2O_2 as a strong oxidizing agent can cause depolymerization of Chi and thus formation of hydroxyl ions and free radicals that initiate oxidation [42]. It has also been reported that Chi can serve as a good solid adsorbent to adsorb enzymes better [43]. Additionally, it was argued that Chi provides a more suitable micro-environment for direct electron transfer between an enzyme and a reactive surface [43]. Therefore, Chi has the potential to improve pixel intensity when used in combination with KI. Both Chi with KI and TMB have been used in μPADs to ensure high sensitivity and low LOD for the detection of glucose [43]. After modification, μPADs were tested with artificial saliva containing glucose at various concentration levels. As it can be seen in Fig. 3, the intensity of color in all three detection zones rised with increasing glucose concentration. However, concentration dependent color change at low levels of glucose was more distinguishable with TMB as compared to the others. Additionally, unlike TMB, both KI and KI+Chi had poor color uniformity within the borders of the detection zones. It is more likely that the test solution flowing through the microchannels dragged both the colorimetric reagents and unbound enzymes in the detection zone, thereby impairing the color homogeneity. Poor color uniformity especially in lateral flow devices is one of the major problems of this technology [44–46]. To address the issue, a custom-designed *GlucoSensing* with an embedded image processing tool [34] was integrated to the server via the cloud system in order to perform machine learning in the colorimetric analysis.

Machine learning methods need to be trained in advance with

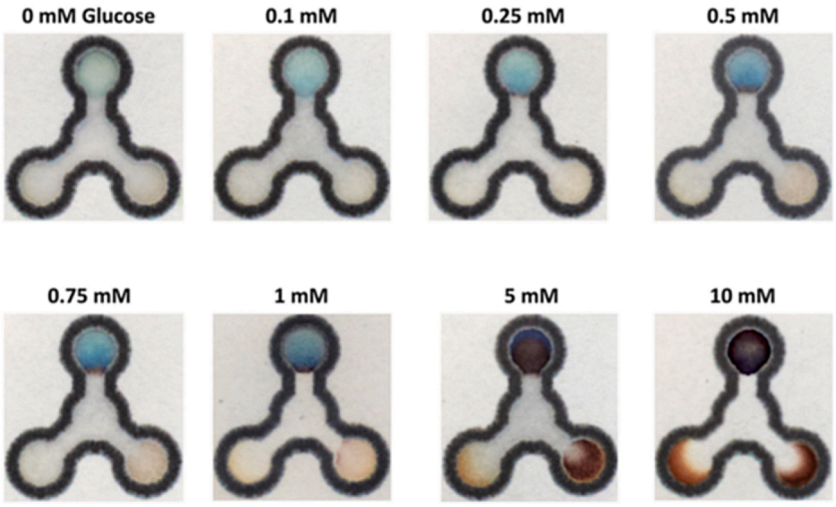

Fig. 3. Color changes observed in μPAD at different glucose concentration levels (top: GOx + HRP + TMB, bottom-left: GOx + HRP + KI, bottom right: GOx + HRP + Chi + KI).

extracted features from the dataset consisting of similar images that the user may use to test. One way to extract features from images is to use color information that can be obtained by image processing as done here. The input image was first cropped to decrease the image size as the user does in *GlucoSensing* (Fig. 2b–d), leading to the cropped patch shown in Fig. 4a. The ROI in the cropped patch needed to be detected for feature extraction in further steps. In that sense, the patch was converted to a grayscale image using the green channel (Fig. 4b) and binarized (Fig. 4c) with a threshold provided by the Otsu method [47]. However, it contained noises (white dots in the black area and black dots in the white area), which were removed by morphological operations (image processing) as shown in Fig. 4d and e. Fig. 4e is noise-free and can be masked with Fig. 4a to get the ROI as shown in Fig. 4f. Figs. 4a to l show the image processing steps applied to the images of 10 mM glucose captured under sunlight. Fig. 4a and g was obtained with the detection mixtures containing KI and KI+Chi, respectively. After the ROI was obtained, 33 features were extracted as described in Section 2.4 to be used in machine learning classifiers. Here, the LDA, GBC and RF classifiers were proposed to use in quantification of glucose content on μPADs and the performance of the classifiers was evaluated by computing classification accuracy (Eq. (1)), precision (Eq. (2)), recall (Eq. (3)) and f1 score (Eq. (4)).

$$\text{Accuracy} = \frac{\text{TP} + \text{TN}}{\text{TP} + \text{TN} + \text{FP} + \text{FN}}, \tag{1}$$

$$\text{Precision} = \frac{\text{TP}}{\text{TP} + \text{FP}}, \tag{2}$$

$$\text{Recall} = \frac{\text{TP}}{\text{TP} + \text{FN}}, \tag{3}$$

$$\text{F1score} = 2 \times \frac{\text{Precision} \times \text{Recall}}{\text{Precision} + \text{Recall}}, \tag{4}$$

TP and TN define the amount of correctly predicted true positive and true negative outputs, respectively whereas FP and FN are the amounts of incorrectly predicted false positive and false negative outputs, respectively. The precision, recall and f1 score evaluate the performance of a classifier statistically by computing the ratio of predicted positive and negative outputs. The precision is the ratio of correctly predicted positives to the total positive predictions while the recall is the ratio of correctly predicted positives to the total true positives and false negatives. Lastly, the harmonic mean of the precision and recall gives the f1 score which has a value between [0, 1] with 1 being the best, and 0 the worst.

Performance comparison of the LDA, GBC and RF classifiers was

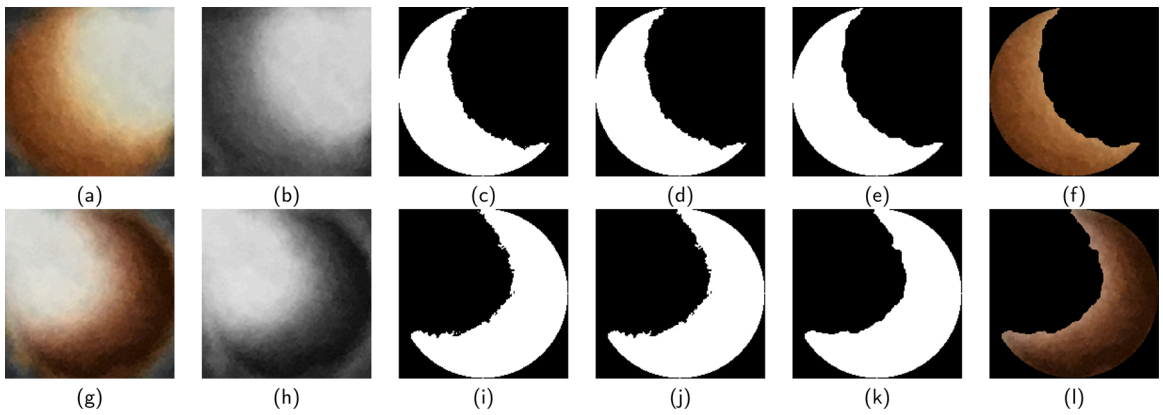

Fig. 4. Image processing steps for 10 mM concentration images captured under sunlight with iPhone 6S. The top row shows the images for KI and the bottom row shows the images for KI+Chi. The cropped patch is given in (a) which is converted to grayscale in (b) and binarized in (c). The noise caused by binarization is removed in (d) and (e) with morphological operations. The noise-free image in (e) is masked with (a) to get the ROI in (f). The same steps are applied for the image in (g) to extract the ROI for KI+Chi in (l).

given in Table 2 which showed that each classifier outperformed the other in different mixtures. The LDA showed the best performance on TMB with 98.24% accuracy while the GBC had the highest accuracy in KI+Chi mixture with 83.04% accuracy. The RF was the first classifier in KI mixture with 76.85% classification accuracy. It is worth mentioning that, classifier performance was improved with the contribution of Chi on the KI mixture on each classifier. However, the best performances for KI and KI+Chi mixtures were limited to 76.83% and 83.04%, respectively. It was mostly because of the less pronounced color transition between successive glucose concentrations.

The performance of classifiers was also evaluated in terms of precision, recall and f1 score. Table 3 shows the results for the LDA. Tables for the RF and GBC were given in the Supplementary data (Tables S1 and S2). Here, "support" defines the number of images for each class. Although the average score was 0.98 for precision, recall and f1, it was variable for each concentration. For clear understanding, confusion matrices were given in Fig. 5a, b and c which visualized the performance of the RF, GBC and LDA in the class base for KI, KI+Chi and TMB, respectively. The confusion matrix is a table that shows the correlation between the true and prediction labels. For example, as can be clearly seen in Table 3, all the scores at 1 mM were lower than the average scores (0.98). The reason can be easily seen in Fig. 5c, where 26 samples out of 28 were correctly classified as 1 mM, while 2 samples were predicted as 0.5 mM.

Lastly, the overall system was integrated with our custom-designed Android application *GlucoSensing* to allow the user to perform a glucose quantification test. Image processing algorithms were embedded to detect the ROI before the image was transferred to the server. Then, the processed image is sent to the server via the Firebase for classification and the result is displayed on the *GlucoSensing* after the concentration level is classified. The smartphone-based platform successfully worked and quantified glucose level in artificial saliva based on machine learning classifiers as expected. The LOD of the sensor with TMB was calculated as 47 μM with an RSD of 4.33% using the RGB data of iPhone 6s obtained under HFS (LOD = $3.3*\sigma$/Slope), which demonstrates the potential of the system to be trained for lower concentrations of glucose.

In addition, the selectivity of the proposed platform was tested in the presence of a number of interfering species including sucrose (0.5 mM), urea (0.5 mM) and lactate (0.5 mM) with 28 images (seven illumination conditions with four smartphones) for each. The platform was able to quantify the glucose concentration level as 0 mM for all images. In other words, the selectivity test was completed with 100% accuracy, which also proved the robustness of the proposed platform.

Table 2
Performance comparison of machine learning classifiers on glucose classification.

	LDA (%)	GBC (%)	RF (%)
TMB	**98.24**	93.30	96.46
KI+Chi	75.45	**83.04**	78.63
KI	74.13	75.98	**76.83**

Table 3
Evaluation of the LDA for TMB in terms of precision, recall and f1 score.

	Precision	Recall	F1-score	Support
0 mM	1.00	1.00	1.00	28
0.1 mM	1.00	1.00	1.00	28
0.25 mM	1.00	1.00	1.00	28
0.5 mM	0.93	0.96	0.95	28
0.75 mM	1.00	1.00	1.00	28
1 mM	0.96	0.93	0.95	28
5 mM	0.97	1.00	0.98	28
10 mM	1.00	0.96	0.98	28
Average	0.98	0.98	0.98	

4. Conclusion

In this study, a new implementation of machine learning classifiers based on a color change in μPADs was proposed to classify glucose level in artificial saliva. Machine learning classifiers were trained using images captured under seven different illumination conditions with four different smartphones, which improved the robustness of the platform against the illumination variance and camera optics. In other words, the current platform is capable of determining the level of glucose in a given sample with very high accuracy regardless of the brand of the smartphone, time and location of the analysis. The platform can also be trained to adapt any other external condition, if required. In addition, a custom-designed smartphone application (*GlucoSensing*) capable of image processing was developed to communicate with the remote server running various machine learning classifiers. The embedded image processing tool in the *GlucoSensing* finds the ROI automatically to minimize human-error, making the platform more user-friendly and precise. Among the tested detection mixtures, the highest classification accuracy was obtained with TMB (98.24%), demonstrating the great advantage of the proposed platform in the colorimetric analysis. To the best of our knowledge, this is the first study that integrates machine learning classifiers and μPAD technology under a smartphone-based platform for glucose quantification. To further improve the classification accuracy, the training dataset can be extended with images captured under diverse light sources with more smartphone brands. The classification sensitivity of the system can also be improved by training the system with closer concentration levels. Lastly, deep learning and transfer learning methodologies could be employed to reach better performance.

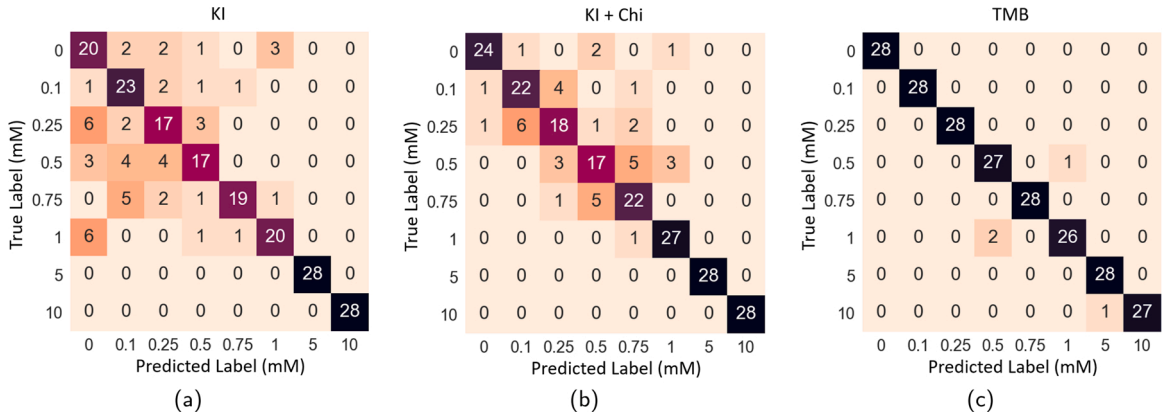

Fig. 5. Confusion matrices of KI, KI+Chi and TMB for the RF, GBC and LDA classifiers, respectively.

Author contribution statement

Öykü Berfin Mercan: Software, investigation, writing – original draft. **Volkan Kiliç:** Software, investigation, writing – original draft, funding acquisition, supervision, project administration. **Mustafa Sen:** Software, investigation, writing – original draft, funding acquisition, supervision, project administration.

Declaration of Competing Interest

The authors report no declarations of interest.

Acknowledgements

This research was supported by the scientific research projects coordination unit of Izmir Katip Celebi University (project nos. 2019-ÖNAP-MÜMF-0004 and 2018-ÖDL-MÜMF-0021) and partly supported by the Scientific and Technical Research Council of Turkey (project nos. 116E934 and 215E003). We also would like to thank Abdurrehim Şen for his guidance in developing the smartphone application.

Appendix A. Supplementary data

Supplementary data associated with this article can be found, in the online version, at https://doi.org/10.1016/j.snb.2020.129037.

References

[1] A.W. Martinez, S.T. Phillips, M.J. Butte, G.M. Whitesides, Patterned paper as a platform for inexpensive, low-volume, portable bioassays, Angew. Chem. Int. Ed. 46 (2007) 1318–1320.
[2] T. Akyazi, L. Basabe-Desmonts, F. Benito-Lopez, Review on microfluidic paper-based analytical devices towards commercialisation, Anal. Chim. Acta 1001 (2018) 1–17.
[3] H. Kettler, K. White, S.J. Hawkes, et al., Mapping the Landscape of Diagnostics for Sexually Transmitted Infections: Key Findings and Recommendations. Technical Report, World Health Organization, Geneva, 2004.
[4] D.M. Cate, J.A. Adkins, J. Mettakoonpitak, C.S. Henry, Recent developments in paper-based microfluidic devices, Anal. Chem. 87 (2014) 19–41.
[5] P. de Tarso Garcia, T.M.G. Cardoso, C.D. Garcia, E. Carrilho, W.K.T. Coltro, A handheld stamping process to fabricate microfluidic paper-based analytical devices with chemically modified surface for clinical assays, RSC Adv. 4 (2014) 37637–37644.
[6] X. Li, J. Tian, T. Nguyen, W. Shen, based microfluidic devices by plasma treatment, Anal. Chem. 80 (2008) 9131–9134.
[7] E. Carrilho, A.W. Martinez, G.M. Whitesides, Understanding wax printing: a simple micropatterning process for paper-based microfluidics, Anal. Chem. 81 (2009) 7091–7095.
[8] Y. Lu, W. Shi, L. Jiang, J. Qin, B. Lin, Rapid prototyping of paper-based microfluidics with wax for low-cost, portable bioassay, Electrophoresis 30 (2009) 1497–1500.
[9] Y. Sameenoi, P.N. Nongkai, S. Nouanthavong, C.S. Henry, D. Nacapricha, One-step polymer screen-printing for microfluidic paper-based analytical device (μpad) fabrication, Analyst 139 (2014) 6580–6588.
[10] X. Li, J. Tian, G. Garnier, W. Shen, Fabrication of paper-based microfluidic sensors by printing, Colloids Surf. B: Biointerfaces 76 (2010) 564–570.
[11] C. Carrell, A. Kava, M. Nguyen, R. Menger, Z. Munshi, Z. Call, M. Nussbaum, C. Henry, Beyond the lateral flow assay: a review of paper-based microfluidics, Microelectron. Eng. 206 (2019) 45–54.
[12] B. Gao, X. Li, Y. Yang, J. Chu, B. He, Emerging paper microfluidic devices, Analyst 144 (2019) 6497–6511.
[13] E.B. Strong, S.A. Schultz, A.W. Martinez, N.W. Martinez, Fabrication of miniaturized paper-based microfluidic devices (micropads), Sci. Rep. 9 (2019) 1–9.
[14] C.-T. Kung, C.-Y. Hou, Y.-N. Wang, L.-M. Fu, Microfluidic paper-based analytical devices for environmental analysis of soil, air, ecology and river water, Sens. Actuators B: Chem. 301 (2019) 126855.
[15] A.F. Coskun, J. Wong, D. Khodadadi, R. Nagi, A. Tey, A. Ozcan, A personalized food allergen testing platform on a cellphone, Lab Chip 13 (2013) 636–640.
[16] A.F. Coskun, R. Nagi, K. Sadeghi, S. Phillips, A. Ozcan, Albumin testing in urine using a smart-phone, Lab Chip 13 (2013) 4231–4238.
[17] H. Zhu, I. Sencan, J. Wong, S. Dimitrov, D. Tseng, K. Nagashima, A. Ozcan, Cost-effective and rapid blood analysis on a cell-phone, Lab Chip 13 (2013) 1282–1288.
[18] A.Y. Mutlu, V. Kılıç, G.K. Özdemir, A. Bayram, N. Horzum, M.E. Solmaz, Smartphone-based colorimetric detection via machine learning, Analyst 142 (2017) 2434–2441.
[19] V. Kilic, G. Alankus, N. Horzum, A.Y. Mutlu, A. Bayram, M.E. Solmaz, Single-image-referenced colorimetric water quality detection using a smartphone, ACS Omega 3 (2018) 5531–5536.
[20] M.-Y. Jia, Q.-S. Wu, H. Li, Y. Zhang, Y.-F. Guan, L. Feng, The calibration of cellphone camera-based colorimetric sensor array and its application in the determination of glucose in urine, Biosens. Bioelectron. 74 (2015) 1029–1037.
[21] M.K. Morsy, K. Zor, N. Kostesha, T.S. Alstrøm, A. Heiskanen, H. El-Tanahi, A. Sharoba, D. Papkovsky, J. Larsen, H. Khalaf, et al., Development and validation of a colorimetric sensor array for fish spoilage monitoring, Food Control 60 (2016) 346–352.
[22] N. Lopez-Ruiz, V.F. Curto, M.M. Erenas, F. Benito-Lopez, D. Diamond, A.J. Palma, L.F. Capitan-Vallvey, Smartphone-based simultaneous ph and nitrite colorimetric determination for paper microfluidic devices, Anal. Chem. 86 (2014) 9554–9562.
[23] Y. Jung, J. Kim, O. Awofeso, H. Kim, F. Regnier, E. Bae, Smartphone-based colorimetric analysis for detection of saliva alcohol concentration, Appl. Opt. 54 (2015) 9183–9189.
[24] C.K. Kuşçuoğlu, H. Güner, M.A. Söylemez, O. Güven, M. Barsbay, A smartphone-based colorimetric pet sensor platform with molecular recognition via thermally initiated raft-mediated graft copolymerization, Sens. Actuators B: Chem. (2019) 126653.
[25] L. Shen, J.A. Hagen, I. Papautsky, Point-of-care colorimetric detection with a smartphone, Lab Chip 12 (2012) 4240–4243.
[26] S. Sumriddetchkajorn, K. Chaitavon, Y. Intaravanne, Mobile device-based self-referencing colorimeter for monitoring chlorine concentration in water, Sens. Actuators B: Chem. 182 (2013) 592–597.
[27] Y. Intaravanne, S. Sumriddetchkajorn, Android-based rice leaf color analyzer for estimating the needed amount of nitrogen fertilizer, Comput. Electron. Agric. 116 (2015) 228–233.
[28] M.E. Solmaz, A.Y. Mutlu, G. Alankus, V. Kilic, A. Bayram, N. Horzum, Quantifying colorimetric tests using a smartphone app based on machine learning classifiers, Sens. Actuators B: Chem. 255 (2018) 1967–1973.
[29] H. Kim, O. Awofeso, S. Choi, Y. Jung, E. Bae, Colorimetric analysis of saliva-alcohol test strips by smartphone-based instruments using machine-learning algorithms, Appl. Opt. 56 (2017) 84–92.
[30] A.K. Yetisen, J. Martinez-Hurtado, A. Garcia-Melendrez, F. da Cruz Vasconcellos, C.R. Lowe, A smartphone algorithm with inter-phone repeatability for the analysis of colorimetric tests, Sens. Actuators B: Chem. 196 (2014) 156–160.
[31] B. Berg, B. Cortazar, et al., Cellphone-based hand-held microplate reader for point-of-care testing of enzyme-linked immunosorbent assays, ACS Nano 9 (2015) 7857–7866.
[32] G.A. Helfer, V.S. Magnus, F.C. Böck, A. Teichmann, M.F. Ferrão, A.B.d. Costa, Photometrix: an application for univariate calibration and principal components analysis using colorimetry on mobile devices, J. Braz. Chem. Soc. 28 (2017) 328–335.
[33] Q. Liu, Y. Liu, F. Wu, X. Cao, Z. Li, M. Alharbi, A.N. Abbas, M.R. Amer, C. Zhou, Highly sensitive and wearable In2O3 nanoribbon transistor biosensors with integrated on-chip gate for glucose monitoring in body fluids, ACS Nano 12 (2018) 1170–1178.
[34] T. Golcez, V. Kilic, M. Sen, A portable smartphone-based platform with an offline image processing tool for rapid paper-based colorimetric detection of glucose in artificial saliva, ChemRxiv, 2020.
[35] Z. Fan, Y. Xu, D. Zhang, Local linear discriminant analysis framework using sample neighbors, IEEE Trans. Neural Netw. 22 (2011) 1119–1132.
[36] A. Natekin, A. Knoll, Gradient boosting machines, a tutorial, Front. Neurorobot. 7 (2013) 21.
[37] U.E. Yildiz, V. Kiliç, Detection of melanoma with multiple machine learning classifiers in dermoscopy images, 2019 Medical Technologies Congress (TIPTEKNO) (2019) 1–4.
[38] F. Elmaz, B. Büyükçakır, Ö. Yücel, A.Y. Mutlu, Classification of solid fuels with machine learning, Fuel 266 (2020) 117066.
[39] G. James, D. Witten, T. Hastie, R. Tibshirani, An Introduction to Statistical Learning, vol. 112, Springer, 2013.
[40] V.K. Aydin, M. Şen, A facile method for fabricating carbon fiber-based gold ultramicroelectrodes with different shapes using flame etching and electrochemical deposition, J. Electroanal. Chem. 799 (2017) 525–530.
[41] K. Ragavan, S.R. Ahmed, X. Weng, S. Neethirajan, Chitosan as a peroxidase mimic: paper based sensor for the detection of hydrogen peroxide, Sens. Actuators B: Chem. 272 (2018) 8–13.
[42] M. Mucha, A. Pawlak, Complex study on chitosan degradability, Polimery-Warsaw 47 (2002) 509–516.
[43] E.F. Gabriel, P.T. Garcia, T.M. Cardoso, F.M. Lopes, F.T. Martins, W.K. Coltro, Highly sensitive colorimetric detection of glucose and uric acid in biological fluids using chitosan-modified paper microfluidic devices, Analyst 141 (2016) 4749–4756.

[44] K. Yamada, T.G. Henares, K. Suzuki, D. Citterio, Paper-based inkjet-printed microfluidic analytical devices, Angew. Chem. Int. Ed. 54 (2015) 5294–5310.
[45] A.K. Yetisen, M.S. Akram, C.R. Lowe, based microfluidic point-of-care diagnostic devices, Lab Chip 13 (2013) 2210–2251.
[46] E. Evans, E.F.M. Gabriel, W.K.T. Coltro, C.D. Garcia, Rational selection of substrates to improve color intensity and uniformity on microfluidic paper-based analytical devices, Analyst 139 (2014) 2127–2132.
[47] H.J. Vala, A. Baxi, A review on Otsu image segmentation algorithm, Int. J. Adv. Res. Comput. Eng. Technol. 2 (2013) 387–389.

Öykü Berfin Mercan received the B.Sc. degree in electrical and electronics engineering from Akdeniz University, Antalya, Turkey, in 2018. She joined the Artificial Intelligence Laboratory in Izmir Katip Celebi University, Izmir, Turkey in 2019 where she is currently pursuing her master degree. Her current research interests include machine learning, deep learning, image processing, colorimetric detection and smartphone sensing.

Dr. Volkan Kılıç received the B.Sc. degree in electrical and electronics engineering from Anadolu University, Eskisehir, Turkey, in 2008. He received the M.Sc. degree in Electronics Engineering from Istanbul Technical University, Institute of Science and Technology, Istanbul, Turkey, and started the Ph.D. in the same university in 2010. He joined the Centre for Vision, Speech and Signal Processing in University of Surrey, Guildford, U.K in 2012 and completed his Ph.D. in 2016. He is currently assistant Professor in Izmir Katip Celebi University, Izmir, Turkey. His current research interests include audio-visual signal processing, image processing, sensor fusion and smartphone sensing.

Dr. Mustafa Sen received his M.Sc. degree in Molecular Biology and Genetics from Istanbul Technical University in 2010 and Ph.D. degree in Bio-engineering from Tohoku University in 2013. He currently works as an Associate Professor at the Department of Biomedical Engineering, Izmir Katip Celebi University. His main research focus is in the field of micro- and nano biosensor development and their applications in single cell and micro-tissue analysis.